

NUMERICAL MODELLING OF A HIGH-PRESSURE TYPE 2 CYLINDER FOR STORING NATURAL GAS FOR VEHICLES

Giselle Barbosa de Mattos, giselle@metal.eeimvr.uff.br

Luiz Carlos Rolim Lopes, rolimlop@metal.eeimvr.uff.br

Anaisa de Paula Guedes Villani, lesa220@yahoo.com.br

Thiago de Carvalho Silva, thiagouffvr@yahoo.com.br

Jayne Pereira de Gouvêa, jpg@metal.eeimvr.uff.br

Luciano Pessanha Moreira, luciano.moreira@metal.eeimvr.uff.br

Universidade Federal Fluminense – Escola de Engenharia industrial Metalúrgica de Volta Redonda – Pós-Graduação em Engenharia Metalúrgica

Adriano de Senne, Adriano_Senne@praxair.com

CILBRÁS – Cilindros S.A.

Abstract. ISO 11439 standard considers 4 types of high-pressure cylinders to store natural gas for vehicles applications. Among them, the type II, metal-lined hoop wrapped cylinder, is the aim of this work. It describes an analytical model built to determine optimal thickness of composite reinforcement applied on the liner by filament winding process, and a numerical model applied to the cylinder. Using design criterion for laminate composites, the total thickness of the composite layer has been evaluated as a function of winding angle. Different composite materials have been studied. For numerical analysis, Finite Element Method was employed using a multilayer shell element of ANSYS - versions 8.1 and 11.0 - the stress state in the metal liner and in each layer of the composite has been studied. The results are analysed considering the performance of the cylinder under test conditions (30 MPa) and work conditions (20 MPa) of loading. In a comparative way, the best results occurs to carbon/epoxy composite, which has the biggest Young's Modulus and failure strength. In this case the modeled thickness was the smallest among the studied materials, and it's on accord with dimensional criterion established by shell theory, besides the carbon/epoxy reinforcement had smallest difference between numerical and analytical results.

Keywords: CNG cylinder; reinforcement; composite; thickness; finite element

1. INTRODUCTION

The ISO 11439 standard admits a sort of 4 different cylinders for Natural Vehicular Gas (CNG or NVG) safe storage. Among them, type 2, metallic steel liner wrapped by spooled long fibers composite – shown in picture 1 – is the focus of this project, which was accomplished due to a partnership of EEIMVR/UFF and White Martins/CILBRÁS. The composite layer wrapped in the type 2 cylinder reinforces and holds the load due to the inner pressure in the metallic liner, in such a way that a thinner metallic wall is allowed (about half the thickness) when compared to a type 1 full metallic cylinder. This allows achieving a lightweight cylinder to resist the specified inner pressures.

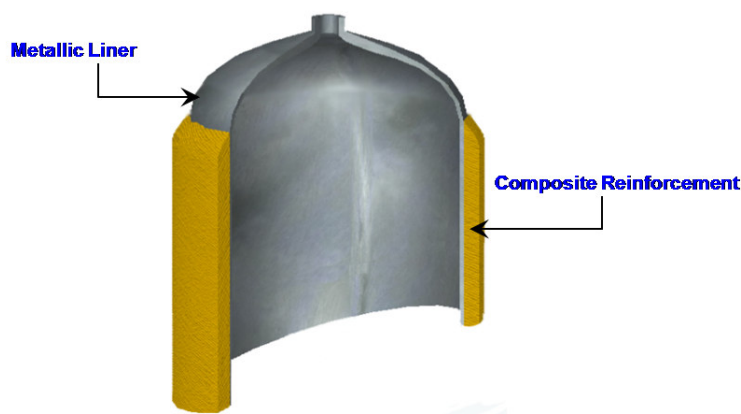


Figure 1. Section view of type 2 cylinder as classified by ISO 11439 standard.

The composite, filament and resin materials selection and the filament winding angle over the metallic liner are extremely important to the cylinder performance, weight and cost. The purpose of this paper is to analyze, compare and select composite materials used as reinforcement as well as the winding pattern. Therefore it has been used an analytical model for thickness optimizing as a function of the winding angle for each material. The numerical model was built

using ANSYS finite elements code to calculate the stress in the metallic liner and composite reinforcement. The results were analyzed on the basis of the cylinder performance when charged in work and test conditions.

2. METHODOLOGY

In this paper, were evaluated cylinders performances with composite reinforcements in different materials, thicknesses and winding angles, to a metallic liner made with low alloy steel 41B30H used in pipe manufacturing which has 4,4 mm thick and internal radius of 162mm. For each model, the methodology described in figure 2 was adopted:

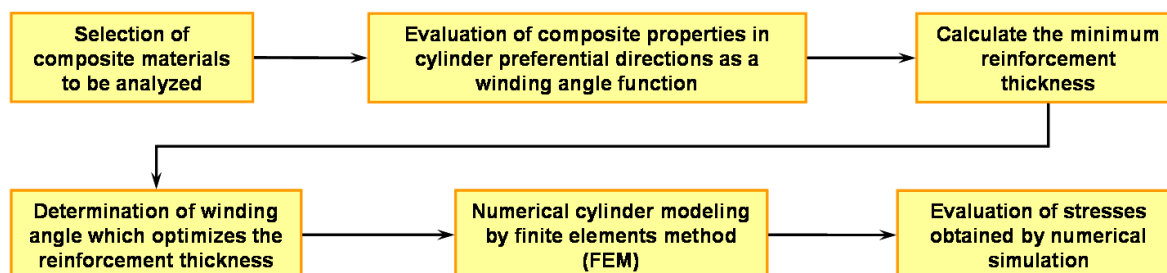


Figure 2. Methodology to build and evaluation of models.

2.1. Materials

The composite materials chosen for this paper are composed by E-glass, aramide (Kevlar) and carbon fiber. In all cases the matrix was an epoxy resin, and the fiber/matrix ratio was the same ($V_f = 60\%$). Tables 1 show the properties of composite materials to be evaluated, and table 2 show metallic liner properties, as hardened and tempered.

Table 1. Mechanical ply properties of composite materials (Gay et. al., 2003, Al-Khalil and Soden, 1994).

| Properties | E glass/Epoxy | Kevlar/Epoxy | Carbon/Epoxy | Observation |
|-----------------------------|---------------|--------------|--------------|--|
| ρ (kg/m ³) | 2080 | 1350 | 1530 | ρ = density or especific mass |
| E_{long} (GPa) | 45,6 | 73,8 | 147 | E_{long} = Young's module in longitudinal direction; |
| E_{transv} (GPa) | 16,2 | 5,20 | 8,12 | E_{transv} = Young's module in transversal direction; |
| ν_{lt} | 0,28 | 0,44 | 0,19 | ν_{lt} = Poisson's ratio in layer plan; |
| G_{lt} (GPa) | 5,50 | 2,59 | 5,52 | G_{lt} = Shear modulus in layer plan; |
| σ_{longR} (MPa) | 1140 | 1400 | 2280 | σ_{longR} = Rupture strength in longitudinal direction; |
| $\sigma_{transvR}$ (MPa) | 39 | 30 | 57 | $\sigma_{transvR}$ = Rupture strength in transversal direction |
| τ_{ltR} (MPa) | 89 | 49 | 76 | τ_{ltR} = Shear strength in the layer plan; |

Table 2. Mechanical properties of AISI 41B30H steel.

| Properties | Steel 41B30H | Observation |
|------------------|--------------|-------------------------------|
| E (GPa) | 210 | E = Young's module; |
| ν | 0,3 | ν = Poisson's ratio; |
| σ_y (MPa) | 815 | σ_y = Yield strength; |
| σ_R (MPa) | 906 | σ_R = Rupture strength |

2.2. Analytical Model of Composite Reinforcement

In order to achieve the composite layer modeling it is necessary to consider a new coordinate system which is compatible with the membrane stress analysis. The adopted system considers the cylinder preferential orientations – (R, ϕ , Z), where directions are, R: radial, ϕ : circumferential and Z: longitudinal – and this is the same one used in the numerical modeling. Figure 3 shows the orientations for the winding direction (θ).

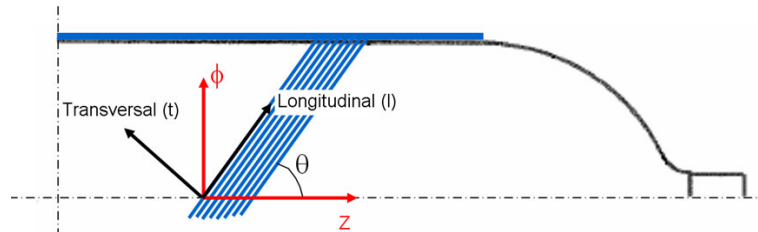


Figure 3. Cylindrical coordinate system (R, ϕ , Z) and fibers orientation related to the cylinder.

The composite properties in new orientation system can be determined by considering the filament winding angle throughout an analytical model (Gay et al., 2003). An important feature in this model is that not only does it consider the material E_{long} and E_{transv} effects but it also considers the G_{lt} e ν_{lt} , as shown in the equations bellow. In these equations “s” and “c” are respectively the sin and the cossin of the winding angle (θ) of the fiber over the metallic liner.

$$E_{\phi}(\theta) = \frac{1}{\frac{s^4}{E_{long}} + \frac{c^4}{E_{transv}} + s^2 \cdot c^2 \left(\frac{1}{G_{lt}} - 2 \frac{\nu_{lt}}{E_t} \right)} \quad (1)$$

$$E_z(\theta) = \frac{1}{\frac{c^4}{E_{long}} + \frac{s^4}{E_{transv}} + s^2 \cdot c^2 \left(\frac{1}{G_{lt}} - 2 \frac{\nu_{lt}}{E_t} \right)} \quad (2)$$

Three models were developed using an unique composite material as a reinforcement in each model. The membrane stresses were obtained by changing the basic equation for this structure, composed by two different materials (Amorim, 2005). The modeled and adopted equations are listed bellow:

For metallic liner:

$$\sigma_{\phi_{liner}} = \frac{p \cdot R}{\left(\frac{E_{composite}}{E_{liner}} \right) \cdot t_{comp} + t_{liner}} \quad (3)$$

$$\sigma_{z_{liner}} = \frac{p \cdot R}{2 \cdot \left[\left(\frac{E_{composite}}{E_{liner}} \right) \cdot t_{comp} + t_{liner} \right]} \quad (4)$$

And for composite reinforcement:

$$\sigma_{\phi_{composite}} = \frac{p \cdot R}{\left(\frac{E_{liner}}{E_{composite}} \right) \cdot t_{liner} + t_{comp}} \quad (5)$$

$$\sigma_{z_{composite}} = \frac{p \cdot R}{2 \cdot \left[\left(\frac{E_{liner}}{E_{composite}} \right) \cdot t_{liner} + t_{comp} \right]} \quad (6)$$

In order to specify the reinforcement thickness it was used the liner yield fail avoidance criteria. In this way the maximum metallic liner stress admitted in the critical direction (radial) will be the steel yield stress divided by a project factor, f_p . And p is the internal pressure, R is the radius of the cylinder, t_{comp} and t_{liner} , are the thickness of the composite and the liner respectively.

$$\sigma_{\phi_{liner}} = \frac{p \cdot R}{\left(\frac{E_{\phi_{comp}}}{E_{liner}} \right) \cdot t_{comp} + t_{liner}} = \frac{\sigma_{y_{AISI\ 41\ B\ 30\ H}}}{f_p} \quad (7)$$

Considering:

$$R = r_{inner} + \frac{t_{comp} + t_{liner}}{2} \quad (8)$$

and defining:

$$K = \frac{\sigma_{y_{AISI\ 41\ B\ 30\ H}}}{f_p \cdot p \cdot E_{liner}} \quad (9)$$

One gets the expression for reinforcement thickness:

$$t_{comp} = \frac{t_1 \cdot (2 E_{liner} \cdot K - 1) - 2 r_{inner}}{1 - 2 \cdot E_{comp} \cdot K} \quad (10)$$

In this paper the project factor (f_p) adopted was 1,33. All the analytical modeling steps were developed for angles between 0° and 90° in $0,5^\circ$ rate. Therefore it is possible to determine the best winding angle by stress minimizing criteria, for circumferential stress.

In numerical model, the best angle for each material will be considered by alternating modeling of negative and positive orientations.

2.3. Numerical model for stress analysis

For the numerical modeling the finite elements code versions 8.1 and 11.0 of ANSYS was adopted in order to calculate the stresses in the metallic liner and in the composite layers. Considering the composite material features such as orthotropy and multilayer, the “shell multilayer” element (SHELL99) was chosen, which allows to insert up to 250 different material layers and their respective thickness and winding angles (Mattos, 2008).

Figure 4 shows a detail of the mesh created in one of the models:

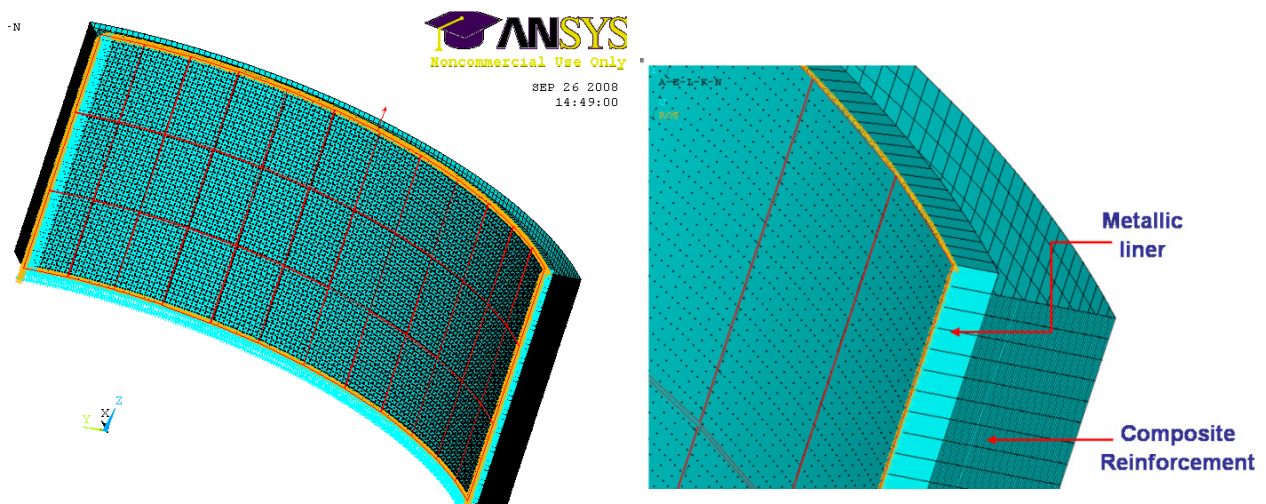


Figure 4. Numerical model and it's detail of the mesh showing the steel inner layer (liner) and the composite layers (reinforcement).

The geometry of numerical model is a reproduction of central portion of reinforced cylinder. Longitudinal stresses caused by cylinder dome (liner dome) must be considered in numerical model, so it's was included during model construction. Table 3 shows the values of these stresses, which was calculated by equation 4, for work and test conditions (internal pressure).

Table 3. Longitudinal stresses applied to numerical model, due to metallic dome effect.

| Material | Longitudinal Stress applied (MPa) | |
|---------------|-----------------------------------|------------------------|
| | Work pressure (20 MPa) | Test pressure (30 MPa) |
| E glass/Epoxy | 189,67 | 284,51 |
| Kevlar/Epoxy | 191,47 | 287,20 |
| Carbon/Epoxy | 194,55 | 291,83 |

The analysis performed by this model has allowed to obtain the equivalent stresses in each layer, which was used to the fail analysis, quite as in the metallic liner as in composite reinforcement.

3. RESULTS AND DISCUSSION

3.1. Analytical modeling of composite reinforcement layer

The first analysis is about the elastic behavior of the different composites studied. Figure 5 shows the variation of Young's module in circumferential direction of cylinder as a function of the winding angle.

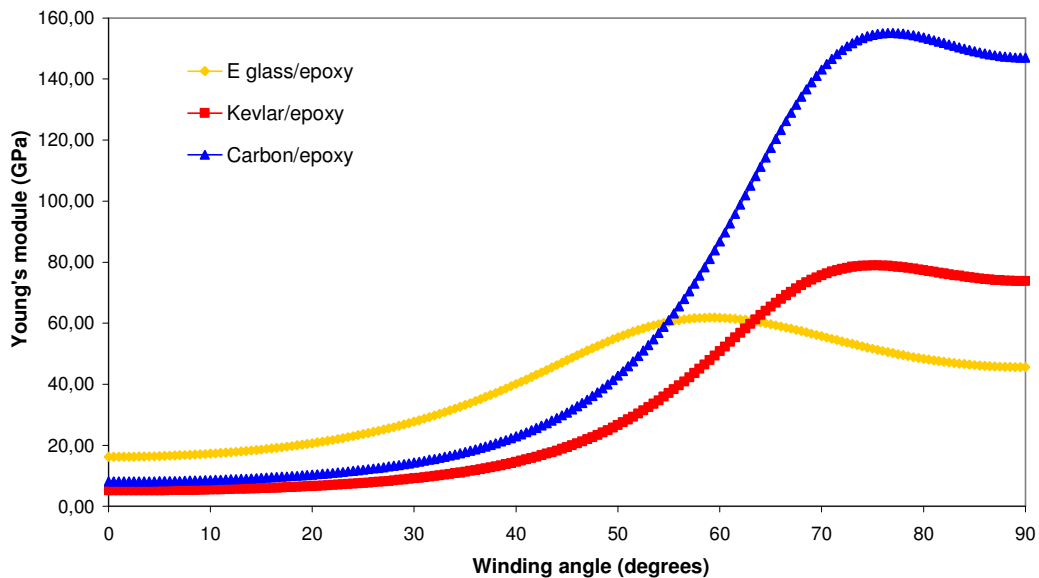


Figure 5. Young's module in circumferential direction for the three to composite materials analyzed.

Notice that for the three materials the Young's module calculated by the equations (1) and (2) reached higher values compared to the longitudinal fiber direction. Its dues to the fact that it considers the E_{long} , E_{transv} , G_{lt} and ν_{lt} effects.

The next step is to calculate the composite thickness for each case, using the criteria described in the equation (10). This equation uses the composite circumferential Young's module ($E_{y_{comp}}$) as the membrane stresses is critical in this direction. Figure 6 shows the variation of the total reinforcement layer thickness as a function of the winding angle, for each composite reinforcement evaluated.

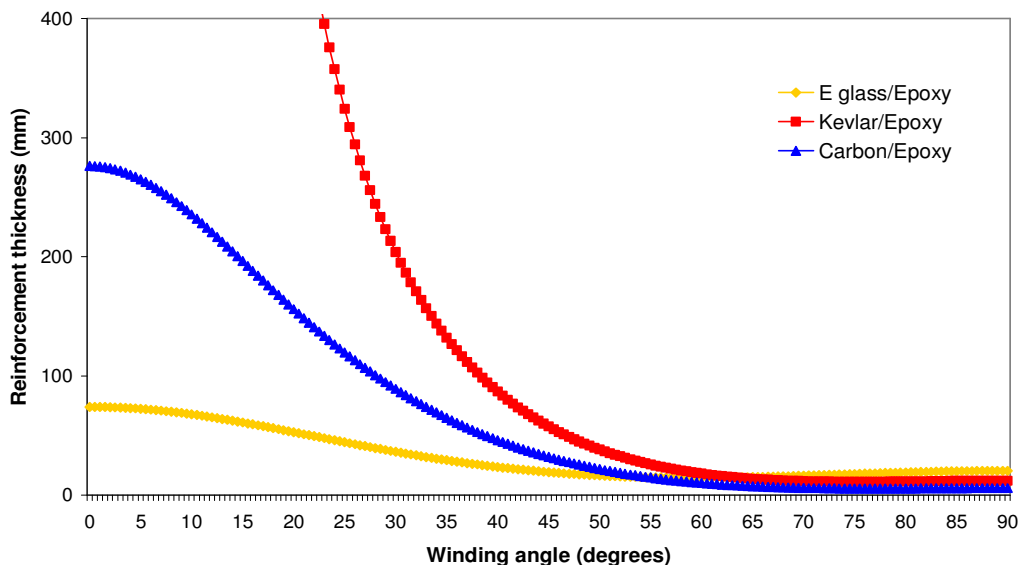


Figure 6. Reinforcement thickness (mm) x θ (degrees) to composite materials analyzed.

This thickness analysis allows finding the optimum orientation, i.e., the one which gives the minimum composite thickness. The table 4 shows the optimum winding angles found for each material and its respective minimum composite thickness.

Table 4. Optimum winding angle and the minimum thickness of reinforcement layer.

| Material | Winding angle(θ) | $t_{\text{reinforc.}}$ | t_{total} | R_{average} | $R_{\text{average}}/t_{\text{total}}$ |
|---------------|---------------------------|------------------------|--------------------|----------------------|---------------------------------------|
| E glass/Epoxy | 59° | 14,46 mm | 18,86 mm | 171,43 mm | 9,09 |
| Kevlar/Epoxy | 74,5° | 11,10 mm | 15,50 mm | 169,75 mm | 10,95 |
| Carbon/Epoxy | 76,5° | 5,47 mm | 9,87 mm | 166,93 mm | 16,91 |

An important result is the ratio between average radius and total thickness of cylinder (liner + reinforcement). For a shell structure, this ratio should be higher than 20 (Ugural, 1981). But as it can be seen in table 4, only carbon/epoxy reinforcement reaches a value close to this. Numerical model was constructed as a shell structure, so the effects of thickness can be evaluated by comparison between numerical and analytical results for circumferential and longitudinal stresses, as will be shown ahead.

The three materials presented very high values for the thickness in a certain winding angle range, and kevlar/epoxy reinforcement presented a winding angle range in which no valid solutions were found. These angle ranges exist because thickness gets so big that the membrane theory used in thickness equation is not valid. The progressive increase in thickness for smaller winding angles characterizes the deviation from membrane structure, and it occurs because for these angles, the Young's module in circumferential direction becomes progressively smaller and to keep the strength the reinforcement layer needs to be thicker.

The elastic properties in optimum winding angle of composites and the thicknesses of reinforcements were used as input data for numerical model.

3.2. Numerical modeling

Results of stress analysis in the composite reinforcement and metallic liner obtained from numerical simulation are presented respectively in tables 5 and 6. For the composites, average stress results for work and test conditions are compared to rupture strength, in order to evaluate how far is the component from rupture. For the liner, both work and test numerical equivalent stresses (von Mises) are compared with yield stress of AISI 41B30H steel presented on table 2.

Table 5. Resume of numerical results to stress analysis – Composite reinforcement.

| Stress | E glass/Epoxy | Kevlar/Epoxy | Carbon/Epoxy |
|--|---------------|--------------|--------------|
| σ_{circumf} (work) | 63,50 MPa | 120,17 MPa | 245,41 MPa |
| σ_{circumf} (test) | 95,25 MPa | 180,26 MPa | 368,11 MPa |
| σ_{circumf} (Rupture strength) | 144,75 MPa | 158,20 MPa | 413,37 MPa |
| $\sigma_{\text{circumf work}}/\text{Rupture strength.}$ | 0,43 | 0,76 | 0,59 |
| $\sigma_{\text{longitudinal}}$ (work) | 11,32 MPa | 9,35 MPa | 12,73 MPa |
| $\sigma_{\text{longitudinal}}$ (test) | 16,98 MPa | 14,03 MPa | 19,09 MPa |
| $\sigma_{\text{longitudinal}}$ (Rupture strength) | 73,01 MPa | 33,01 MPa | 61,06 MPa |
| $\sigma_{\text{longitud work}}/\text{Rupture strength.}$ | 0,15 | 0,28 | 0,21 |
| σ_{shear} (work) | 18,97 MPa | 27,96 MPa | 50,47 MPa |
| σ_{shear} (test) | 28,45 MPa | 41,93 MPa | 75,71 MPa |
| σ_{shear} (Rupture strength) | 43,47 MPa | 127,00 MPa | 104,98 MPa |
| $\sigma_{\text{shear work}}/\text{Rupture strength.}$ | 0,44 | 0,22 | 0,48 |

Table 6. Resume of numerical results to stress analysis – Metallic liner.

| Stress | Liner _{E glass/epoxy} | Liner _{Kevlar/epoxy} | Liner _{Carbon/epoxy} |
|---|--------------------------------|-------------------------------|-------------------------------|
| $\sigma_{\text{circumferential}}$ (work) | 498,26 MPa | 403,74 MPa | 394,25 MPa |
| $\sigma_{\text{circumferential}}$ (test) | 747,36 MPa | 601,11 MPa | 591,38 MPa |
| $\sigma_{\text{longitudinal}}$ (work) | 362,73 MPa | 296,36 MPa | 201,63 MPa |
| $\sigma_{\text{longitudinal}}$ (test) | 544,10 MPa | 441,54 MPa | 302,45 MPa |
| $\sigma_{\text{equivalent work}}$ (máx selante) | 494,42 MPa | 392,95 MPa | 378,57 MPa |
| $\sigma_{\text{equivalent test}}$ (máx selante) | 741,62 MPa | 589,42 MPa | 567,86 MPa |
| $\sigma_{\text{equivalent work}}/\sigma_{\text{y AISI 41B30H}}$ | 0,60 | 0,48 | 0,46 |
| $\sigma_{\text{equivalent test}}/\sigma_{\text{y AISI 41B30H}}$ | 0,90 | 0,72 | 0,69 |

Comparing results for stresses for work and test conditions can be seen that is a difference about 50% between the numerical values. These results indicate that numerical model (with its specific approximation methods) is representative from real situation, therefore reflect the difference between work and test pressures.

Values of rupture strength presented on table 5 for circumferential and longitudinal directions, and for shear plane were obtained by application of specific equations for properties rotation. It can be noted, although circumferential stress on test condition for kevlar/epoxy reinforcement is an exception, in other cases none of the composites reaches its respective rupture strength in any layer that make's up the reinforcement, then keeping itself in the elastic behavior for both conditions of pressurization.

Orthotropic behavior of composite reinforcement had generated different ratios between longitudinal and circumferential for each analyzed composite. These results show the effects of difference on properties in orthotropic directions. As show on table 1, carbon reinforcement has the biggest difference between orthotropic properties, which was observed for numerical stresses results.

The maximum equivalent stresses obtained on simulations were, as shown in table 6, all smaller than the value of yield stress of the metal liner is made. Thus, according to von Mises criterion, the yield stress is not achieved, either in conditions of work ($p = 20$ MPa) or test ($p = 30$ MPa) for all composite materials studied. The analysis of the ratios of

equivalent stress to yield stress, for three composite materials, showed that carbon/epoxy has the best performance, because it is the reinforcement that provides the lowest levels of equivalent stresses on liner.

Also, it can be observed in table 6 that the values of stresses acting on liner are much larger than those for composite reinforcements. Comparing the values for circumferential stresses on tables 5 and 6, one can see that the difference in stress level in the liner and in the composite is more pronounced for E glass/epoxy reinforcement, followed by kevlar/epoxy and then carbon/epoxy. This difference is an indicative of how stresses are distributed between liner and reinforcement. For carbon/epoxy, which has the higher Young modulus the composite is responsible for supporting a significant portion of circumferential stresses. Reinforcements with lower modulus, mainly Eglass/epoxy, despite its largest thickness induces higher stress in liner.

Table 7 presents a comparison between the numerical and analytical results for stress in the liner for the three composite materials. From these results it can be note two points. The first one is the differences between the numerical and calculated stress by means of the membrane equations (3) and (4). The second one comes from the membrane theory statement by which $\sigma_{\text{longitudinal}} = 0,5 \cdot \sigma_{\text{circumferential}}$. From table 7 one can see that carbon/epoxy composite material is the one which shows the least difference between numerical and analytical results and approaches the membrane condition of $\sigma_{\text{longitudinal}} = 0,5 \cdot \sigma_{\text{circumferential}}$. Both this two effects can be attributed to the deviation from the membrane condition as thickness of the composite reinforcement increases (see $R_{\text{average}}/t_{\text{total}}$ in table 4).

Table 7 – Stresses in metallic liner: analytical and numerical results.

| ANALYTICAL RESULTS | | | |
|---|--------------------------------|-------------------------------|-------------------------------|
| Stress | Liner _{E glass/epoxy} | Liner _{Kevlar/epoxy} | Liner _{Carbon/epoxy} |
| $\sigma_{\text{circumferential}}$ (work) | 379,35 MPa | 382,93 MPa | 389,11 MPa |
| $\sigma_{\text{circumferential}}$ (test) | 569,02 MPa | 574,40 MPa | 583,66 MPa |
| $\sigma_{\text{longitudinal}}$ (work) | 189,67 MPa | 191,47 MPa | 194,55 MPa |
| $\sigma_{\text{longitudinal}}$ (test) | 284,51 MPa | 287,20 MPa | 291,83 MPa |
| NUMERICAL RESULTS | | | |
| Stress | Liner _{E glass/epoxy} | Liner _{Kevlar/epoxy} | Liner _{Carbon/epoxy} |
| $\sigma_{\text{circumferential}}$ (work) | 498,26 MPa | 403,74 MPa | 394,25 MPa |
| $\sigma_{\text{circumferential}}$ (test) | 747,36 MPa | 601,11 MPa | 591,38 MPa |
| $\sigma_{\text{longitudinal}}$ (work) | 362,73 MPa | 296,36 MPa | 201,63 MPa |
| $\sigma_{\text{longitudinal}}$ (test) | 544,10 MPa | 441,54 MPa | 302,45 MPa |
| STRESSES RATIOS – NUMERICAL RESULTS | | | |
| Ratio | Liner _{E glass/epoxy} | Liner _{Kevlar/epoxy} | Liner _{Carbon/epoxy} |
| $\sigma_{\text{longit}} / \sigma_{\text{circumf}}$ (work) | 0,728 | 0,734 | 0,511 |
| $\sigma_{\text{longit}} / \sigma_{\text{circumf}}$ (test) | 0,728 | 0,734 | 0,511 |
| NUMERICAL / ANALYTICAL DIFFERENCES (%) | | | |
| Stress | Liner _{E glass/epoxy} | Liner _{Kevlar/epoxy} | Liner _{Carbon/epoxy} |
| $\sigma_{\text{circumferential}}$ (work) | +31,3% | +5,43% | +1,32% |
| $\sigma_{\text{circumferential}}$ (test) | +31,3% | +4,65% | +1,32% |
| $\sigma_{\text{longitudinal}}$ (work) | +91,2% | +54,8% | +3,64% |
| $\sigma_{\text{longitudinal}}$ (test) | +91,2% | +53,73% | +3,64% |

As a first analysis can notice a big difference between the stresses calculated by membrane theory for kevlar/epoxy and E glass/epoxy reinforcements, when compared with the results obtained numerically, and same not happens to carbon/epoxy.

Another important point is that for membrane theory (equations 3 to 6), the proportion between the longitudinal and circumferential stresses in this kind of structure is 50% ($\sigma_{\text{longit}} = 0,5 * \sigma_{\text{circumf}}$). However, the results in third part of table 7 again show that to E glass/epoxy and kevlar/epoxy this ratio is not achieved by numerical results, but only to carbon/epoxy reinforcement. This material, as shown in table 4, has the smaller thickness and is nearest of geometric condition for membrane structure (thin wall). When coated with any of the other two composites, that have thicker reinforcements, the stresses relationship exceeds the theory expectation, but despite the differences in mechanical properties and thicknesses, the stresses ratio were very close to E glass/epoxy and kevlar/epoxy. This result shows a possible similarity between structural behavior in these cases.

The fourth part of table 10 reinforces the view that carbon/epoxy is the reinforcement closer of membrane structure, cause as can be seen the differences between the numerical and analytical results obtained with carbon/epoxy are lower. Whereas the basis of analytical calculations was the theory of thin-walled shells, and more specifically, the membrane stresses, and that in numerical evaluation this condition is not directly imposed to the model, is consistent for the cases where thickness was higher (E glass and kevlar) there is a more pronounced difference between numerical and analytical results.

It should also take into account that classical membrane theory does not consider the properties of material that composes the shell, only internal pressure and dimensional features (shell thickness). Also, it was developed for isotropic materials. This study evaluates multilayer and multi material shells. The modeled membrane stresses (equations 3 to 6) include Young modulus of materials that make up the different portions of NVG cylinder. For the steel liner isotropic material there is an unique elastic property. But for orthotropic reinforcement is necessary introduce some new considerations as the use of circumferential Young modulus of composite, given the larger stress level for this direction, which is critical to crack growth in liner. When ratio between modulus of the reinforcement and the liner becomes closer of the unit, analytical modeled equations tend to basic membrane theory. So, as carbon ($E_{\text{circumf}} = 155095,1$ MPa by equation 1 and figure 5) being the closest to steel ($E = 210000$ MPa, as table 2) one can see a better performance with respect to membrane theory.

In numerical model the efforts resulting from internal pressure are shared between two materials with diversified mechanical characteristics, and the behavior will be displayed different. Solid continuity is a condition for multilayer shells, so there is consequently an influence of one material on the other. As the carbon/epoxy modulus is higher and therefore approach the modulus of the steel, this composite material contributes to a better sharing of loads with the liner.

4. CONCLUSIONS

- The observation of behavior of curves, thickness x winding angle, for the three tested composites shows a strong influence of difference between longitudinal and tranverse properties for these materials. The bigger is the difference in orthotropic properties, the more pronounced is the gradual change on thickness.
- With respect to evaluated composite materials, can be concluded that the carbon/epoxy offers a better range of properties and advantages, and it's because it reaches the condition of the membrane stress state, supports higher stresses levels when compared to the other options, beyond provides the greatest reduction of cylinder weight in relation to cylinder type I - fully metallic.
- Due to properties much lower than those of steel, the composites kevlar/epoxy and E glass/epoxy demand a total thickness of the reinforcement layer large when compared to the thickness of the metallic liner. Together, these thicknesses distancing the component of the dimensional requirement for structures such as thin-walled shell, which characterized this type of pressure vessel.

5. REFERENCES AND BIBLIOGRAPHY

ISO 11439 Standard – “High Pressure Cylinders for the on-board storage of natural gas as a fuel for automotive vehicles”, ISO/TC 58/SC 3/WG17.

Gay, D.; Hoa, S. V.; Tsai, S.W., “Composite Materials – Design and Applications”, CRC Press, 1st Edition, 2003.

Al-Khalil, M.F.S.; Soden, P.D.; “Theoretical through-thickness elastic constants for filament-wound tubes”, *International Journal of Mechanical Sciences*, Vol. 36, N° 1, 1994, pp. 49-62

- Amorim, G.B.; “Stress analysis in reinforced cylinders to Natural Vehicular Gas (NVG) storage”; Theoretical Doctoral Qualification; Program of Postgraduate in Metallurgical Engineering – UFF-EEIM/VR, Volta Redonda - RJ, Brazil, 2005. pp. 6-10.
- Mattos, G.B.; “Analytical and numerical study of mechanical behavior of type II cylinder for NGV storing and transporting”, Master degree dissertation, Program of Postgraduate in Metallurgical Engineering – UFF-EEIM/VR, Volta Redonda - RJ, Brazil, 2008.
- Ugural, A.C.; “Stresses in Plates and Shells”; McGraw-Hill Book Company, 1st Edition, 1981
- Daniel, I.M.; Ishai, O.; “Engineering Mechanics of Composite Materials”; Oxford University Press, 2nd Edition, 2006, pp. 105 – 109 and 273-282.
- Shen, F.C.; “A filament-wound structure technology overview”, Materials Chemistry and Physics, Vol. 42, 1995, pp. 96-100.
- Callister JR., W.D.; “Materials Science and Engineering: An Introduction”; LTC Press, 5th Edition, 2002, pp. 363.
- Levy Neto, F.; Pardini, L.C.; “Compósitos Estruturais – Ciência e Tecnologia”; Editora Edgard Blücher, 1^a Edição, 2006, p. 5.
- Owen, M.J.; Middleton, V.; Jones, I.A.; “Integrated Design and Manufacture using Fibre-reinforced Polymeric Composites”; CRC Press, 1st Edition, 2000, pp. 237, 349-350.
- Crawford, R.J.; Benham, P. P.; “Mechanics of Engineering Materials”, John Wiley & Sons Press, 1987, p. 331-347.
- Webster, C.; “Taking new approaches in standards development for products for new market – The development of ISO 11439 for compressed natural gas vehicle cylinders”, ISO Bulletin, pp. 71, 2001.
- Walker, M.; Smith, R.; “A methodology to design fibre reinforced laminated composite structures for maximum strength”, Composites – Part B: Engineering, Vol. 34, 2003, pp. 209-214.
- Su, B.; Bhuyan, G.S.; “Effect of composite wrapping on the fracture behavior of the steel-lined hoop-wrapped cylinders”, International Journal of Pressure Vessels and Piping, Vol. 75, 1998, pp. 931-937.
- Carroll, M.; Ellyin, F.; Kujawski, D.; Chiu, A.S.; “The rate-dependent behavior of $\pm 55^\circ$ filament-wound E-glass-fibre/epoxy tubes under biaxial loading”, Composites Science and Technology, Vol. 55, 1995, pp. 391-403.
- Soden, P.D.; Kitching, R.; Tse, P.C.; Tsavalas, Y.; “Influence of winding angle on the strength and deformation of filament-wound composite tubes subjected to uniaxial and biaxial loads”, Composites Science and Technology, Vol. 46, 1993, pp. 363-378.
- Faupel, J.H.; Engineering Design – A synthesis of stress analysis and materials engineering, John Wiley & Sons Press, New York, USA, 1964, pp. 655-709.